

# Nb<sub>3</sub>Sn Wires for the Future Circular Collider at CERN: Microstructural Investigation of Different Wire Layouts

Alice Moros , Mattia Ortino , Stefan Löffler , Maxim Alekseev, Anastasiia Tsapleva , Pavel Lukyanov, Ildar M. Abdyukhanov , Victor Pantyrny, Simon C. Hopkins , Michael Eisterer , Michael Stöger-Pollach, and Johannes Bernardi 

**Abstract**—In the challenging project concerning the realization of the CERN Future Circular Collider (FCC), Nb<sub>3</sub>Sn represents the best candidate material for the construction of high-field superconducting dipole magnets, since it is able to satisfy the requirements of  $J_c$  (non-Cu) = 1.5 kA/mm<sup>2</sup> at 16 T and 4.2 K. In that context, a cluster layout of prototype internal tin Nb<sub>3</sub>Sn wires, developed by TVEL and the Bochvar Institute (Russia), was analyzed and compared to a standard layout produced by the same manufacturer. The main reason for dividing the sub-element into clusters is reducing the effective sub-element size ( $d_{eff}$ ). The microstructural characterization of such a wire layout can provide fundamental contributions to steer the manufacturing processes towards higher performing wires. In particular, since the homogeneity in Sn concentration influences the superconducting properties, the effect of cluster and standard layouts on the Sn concentration gradient over the wire cross-section was evaluated. For this purpose, energy dispersive X-ray (EDX) spectroscopy was employed with both scanning electron microscopy (SEM) and transmission electron microscopy (TEM). Finally, scanning Hall probe microscopy (SHPM) measurements were performed to understand how these cluster wire sub-elements, with their specific geometry, influence the local currents flowing through the wire cross-section on a microscopic scale. The comprehension of the correlation between the microstructural characteristics and superconducting performance is crucial for obtaining wires meeting the requirements of FCC dipole magnets.

**Index Terms**—Critical current density, Future Circular Collider, Nb<sub>3</sub>Sn wire layout, Sn concentration gradient.

Manuscript received November 28, 2020; revised February 4, 2021, February 28, 2021, March 7, 2021, and March 9, 2021; accepted March 12, 2021. Date of publication March 17, 2021; date of current version May 20, 2021. This work was supported in part by Marie Skłodowska-Curie Action EASITrain (European Advanced Superconductivity Innovation and Training), in part by European Union's H2020 Framework Programme under Grant Agreement 764879 and in part by the development of wires by the Bochvar Institute (addenda KE2968 and KE4037) and their characterisation at TU Wien (addendum KE3194) was supported by CERN in the context of the FCC Study. (Corresponding author: Alice Moros.)

Alice Moros, Stefan Löffler, Michael Stöger-Pollach, and Johannes Bernardi are with Technische Universität Wien (TU Wien), USTEM, 1070 Vienna, Austria (e-mail: alice.moros@tuwien.ac.at).

Mattia Ortino and Michael Eisterer are with TU Wien, ATOMINSTITUT, 1020 Vienna, Austria.

Maxim Alekseev, Anastasiia Tsapleva, Pavel Lukyanov, Ildar M. Abdyukhanov, and Victor Pantyrny are with A. A. Bochvar High-Technology Research Institute on Inorganic Materials, 123060 Moscow, Russia.

Simon C. Hopkins is with the European Organization for Nuclear Research (CERN), 1211 Meyrin, Switzerland.

Color versions of one or more figures in this article are available at <https://doi.org/10.1109/TASC.2021.3066541>.

Digital Object Identifier 10.1109/TASC.2021.3066541

## I. INTRODUCTION

THE European Organization for Nuclear Research (CERN) recently published a conceptual design study for a future hadron collider (FCC-hh). This study aims at building a 100 km long tunnel and increasing the collision energy up to 100 TeV, thanks to two counter rotating proton beams with an energy of 50 TeV each. For such a magnificent machine, high performance superconducting bending magnets with a nominal dipole field of 16 T are required: this is about twice the 8.3 T generated by the Nb-Ti magnets in the LHC and about 5 T higher than the 11T of the Nb<sub>3</sub>Sn-based dipole magnet of the high-luminosity (HL) LHC upgrade [1]. Nb<sub>3</sub>Sn, already being produced for the magnets of the upcoming HL-LHC, is currently the only affordable superconducting material that can lead to conductors delivering a critical current density ( $J_c$ ) of at least 1500 A/mm<sup>2</sup> at 4.2 K and 16 T [2]. The state-of-the-art internal tin restacked-rod-process (RRP) Nb<sub>3</sub>Sn wires can reach a  $J_c$  between 1000 A/mm<sup>2</sup> and 1200 A/mm<sup>2</sup> at the before mentioned conditions. Researchers and industrial partners are therefore collaborating in developing and studying innovative wire manufacturing technologies to achieve a higher  $J_c$  performance.

Among the different ways to help the  $J_c$  enhancement, the reduction of inhomogeneities in terms of Sn concentration gradient is one important goal to be reached. In fact, the Nb<sub>3</sub>Sn wires are typically subjected to compositional gradients due to their production method, which influences their superconducting behaviour [3]–[5].

In this work, the Sn gradient was investigated through the analysis of a prototype internal tin Nb<sub>3</sub>Sn wire with a cluster layout (T3 in Fig. 1a), manufactured with the aim of reducing the effective sub-element size ( $d_{eff}$ ). Previous research works aimed at exploring the effectiveness of dividing the sub-element into clusters to reduce  $d_{eff}$  and magnetization effects, starting with the studies by B. A. Zeitlin, E. Gregory *et al.* [6]–[8] and up to the recent one by P. A. Lukyanov *et al.* [9]. In the present work, the impact of the wire cluster configuration on the Sn concentration gradient was investigated and compared to a standard wire layout (T4 in Fig. 1a) reacted with the same heat treatment.

Since this cluster configuration shows three free routes for Sn to diffuse through the Cu matrix during the heat treatment (Fig. 1b), it seems reasonable to think that improvements in

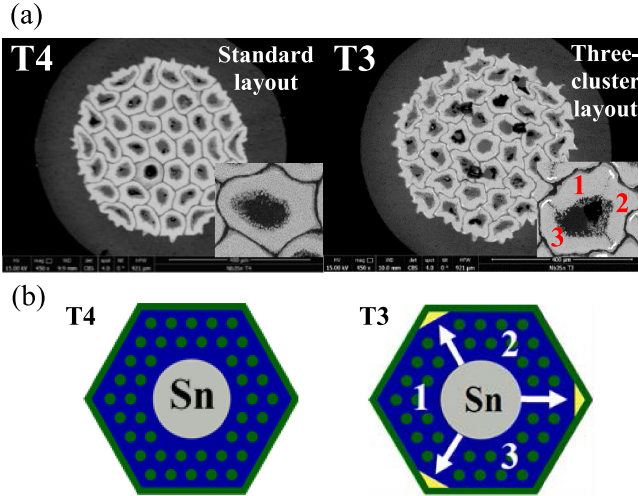


Fig. 1. (a) SEM overview images of a standard wire layout (T4) and a three-cluster wire layout (T3) developed by the Bochvar Institute in Russia. At the bottom right of both images, the details of the sub-element structure are shown. (b) Schematic of the T4 and T3 sub-element starting layouts before heat treatment.

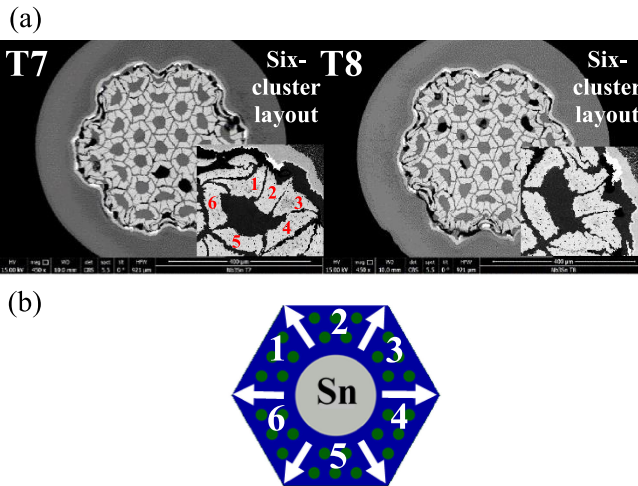


Fig. 2. (a) SEM overview images of the six-cluster wire layout (T7 and T8) developed by the Bochvar Institute in Russia. At the bottom right of both images, the details of the sub-element structure are shown. (b) Schematic of the T7 and T8 sub-element starting layout before heat treatment.

terms of more homogenous Sn distribution over the wire cross-section can be attained. Moreover, the presence of free diffusion pathways may lead to higher Sn content in the peripheral region of the sub-element, which is usually Sn poor.

This study aims at demonstrating the above raised hypotheses, also giving a preliminary idea about the transport properties of the cluster specimen.

To further explore the potential of cluster layouts, two wires presenting the same cluster configuration (see Fig. 2), different from the one previously described, and produced with a different heat treatment were compared in terms of Sn concentration gradient. We could therefore face the inhomogeneity problem from another perspective, not only related to another cluster layout type but also highly influenced by the heat treatment.

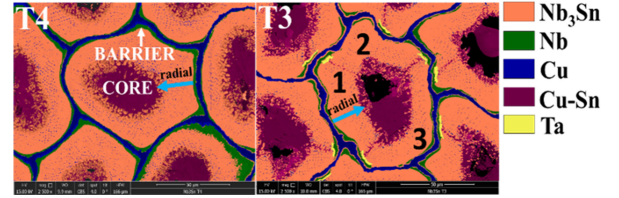


Fig. 3. Close-up of the sub-element configuration details for the standard wire (T4) and the three-cluster one (T3). The light blue arrow represents a typical EDX measurement line from the Nb barrier to the Cu-Sn core.

TABLE I  
STANDARD AND THREE-CLUSTER WIRE FEATURES

Wire identification	Standard layout (T4)	Three-cluster layout (T3)
Wire Ø [mm]	0.7	0.7
Barrier	Distributed Nb	Distributed Nb + Ta-insertions
Dopant	Ti	Ti
Cu-non-Cu ratio	1.3	1.15
Heat treatment	210 °C, 50 h / 400 °C, 50 h / 665 °C, 50 h	210 °C, 50 h / 400 °C, 50 h / 665 °C, 50 h

TABLE II  
SIX-CLUSTER WIRE FEATURES

Wire identification	Six-cluster layout (T7)	Six-cluster layout (T8)
Wire Ø [mm]	0.7	0.7
Barrier	Common Nb + Ta-insertions	Common Nb + Ta-insertions
Dopant	Ti	Ti
Cu-non-Cu ratio	1.2	1.2
Heat treatment	200 °C, 24 h / 380 °C, 50 h / 570 °C, 112 h / 660 °C, 100 h	380 °C, 48 h / 580 °C, 48 h / 700 °C, 92 h

## II. EXPERIMENTAL

### A. SEM-EDX Analysis

The four wires shown above were prepared and investigated by SEM-EDX at USTEM, TU Wien. They were first embedded in a proper epoxy resin and then polished with different roughness Aluminum Oxide discs (from 9 µm to 1 µm). The EDX line scans were performed over several wire sub-elements along the radial direction, from the Nb barrier to the Cu-Sn core, as shown in Fig. 3 through the light blue arrows. A statistical analysis was thus carried out for all the samples, so evaluating and comparing the Sn concentration gradients of T3 and T4 first, respectively cluster and standard wire coming from the same heat treatment, and afterwards those of T7 and T8, the same cluster layout wires produced with different heat treatments. Table I and Table II show the features of T3 and T4 and those of T7 and T8, respectively. For the T3 and T4 EDX line scans, the thickest area per analyzed sub-element was chosen. For the T7 and T8 cases, since each sub-element is divided into six clusters, the EDX line scans were performed and averaged for three clusters per selected sub-element.

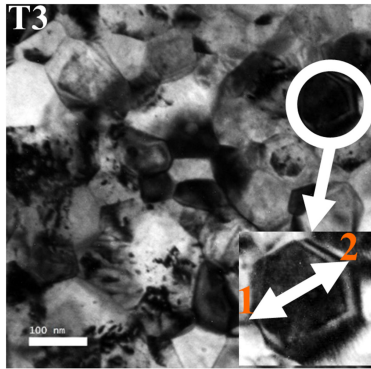


Fig. 4. STEM image showing different T3 Nb<sub>3</sub>Sn grains. The close-up at bottom right is showing a typical EDX line measurement, from one grain boundary (1) to the opposite one (2).

### B. TEM-EDX Analysis

A preliminary TEM-EDX analysis of the cluster sample T3 was accomplished at USTEM to obtain a first indicative confirmation of the results achieved by SEM-EDX. A lamella sample of about 100 nm thickness was prepared by Focused Ion Beam (FIB) and analyzed in STEM mode with a spatial resolution below 10 nm for evaluating the Sn concentration gradient across the Nb<sub>3</sub>Sn grains.

In particular, TEM-EDX line scans were performed over several grains from one grain boundary to the opposite one, as shown in Fig. 4. Considering that grain morphology is closely related to Sn content and the latter is higher in equiaxed grains [10]–[12], approximately round-shaped grains were selected. For such measurements, very thin lamella regions were chosen (approximately 50 nm) to avoid grains overlapping. As for the previous SEM investigation, a Sn gradient statistical analysis was carried out.

### C. Preliminary $J_c$ measurements

The performance of wires characterized by sub-elements with the same standard structure as T4, and produced by the same manufacturer, proved to have comparable  $J_c$  to the HL-LHC specification [13].

As a first step to have a feel for the three-cluster layout transport performance, the T3 local properties were evaluated by SHPM remanent-field scans at Atominstutit, TU Wien. In this way, the influence of the sub-element geometry was evaluated.

Scanning a Hall probe across the surface of a superconductor allows a magnetic field map to be recorded. Remanent-field scans require the magnetization of the sample, made by applying and removing a field of 2 T, resulting in a spatially resolved map of the remanent magnetic field.

These magnetic field maps offer the opportunity to extract the current flow inside the sample by means of inversion of the Biot-Savart law. This analysis depends on several parameters and it is as accurate as the prepared sample is thin. The sample prepared for the measurements was 0.8 mm thick. The T3 current densities profile was evaluated at 10 K and self-field.

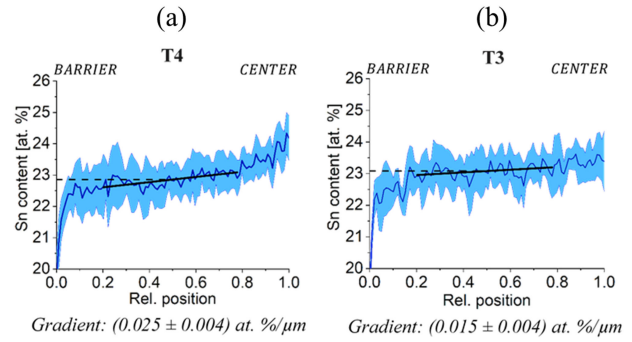


Fig. 5. Sn content gradient along the radial direction, from the Nb barrier to the Sn-Cu core, for both the standard wire T4 (a) and the cluster wire T3 (b). The coloured background stems from the single measurements performed over several sub-elements. The dashed lines represent the average Sn content [at.%] value taken at 0.5.

Results in the literature comparing six-cluster wires (like T7 and T8) to standard wires (like T4) showed that the latter have higher  $J_c$  values [9]. The authors attributed this to compositional factors and microstresses [9], but it should be noted that results for different sub-element designs and heat treatments are not directly comparable.

## III. RESULTS AND DISCUSSION

### A. Sn Concentration Gradients By SEM-EDX

By comparing the three-cluster wire T3 to the standard one T4 (Fig. 5a), the Sn concentration gradient was found to be smaller for the T3 (Fig. 5b): in both standard and cluster cases, the slope of the Sn gradient is slightly ascending towards the core at the limit of the measurement accuracy, but it is more pronounced in the case of the T4.

This work shows that the T3 Sn gradient is reduced by a factor of 1.6 with respect to the T4 one.

The Sn content [at%], which plays an important role in the  $J_c$  enhancement [3], [14], shows its average value taken at 0.5 to be higher for the cluster wire than for the standard one within the experimental margin of error. The cluster sub-elements seem thus to have a great potential in terms of producing wires with higher homogeneity, which can lead to better superconducting performance.

These results let us think that cluster layouts with a higher number of clusters, therefore more free routes for the initial Sn to diffuse towards the barrier, could bring other improvements in terms of a more homogeneous Sn distribution. For this to be better understood, T7 and T8 were analyzed and compared the same way as done for T3 and T4. Since these two wires, showing the same six-cluster layout, were produced with a different heat treatment, the impact of the latter on the Sn concentration gradient was evaluated as well. The related graphs are shown in Fig. 6. For both wires, the slope of the Sn gradient is slightly descendent at the limit of the measurement accuracy and it is more pronounced in the case of the T7, suggesting a more homogeneous Sn distribution over the T8 cross-section.

Despite the noise, due to the presence of Cu inclusions in the Nb<sub>3</sub>Sn volume, the T8 data resembling a slight “U” trend seem

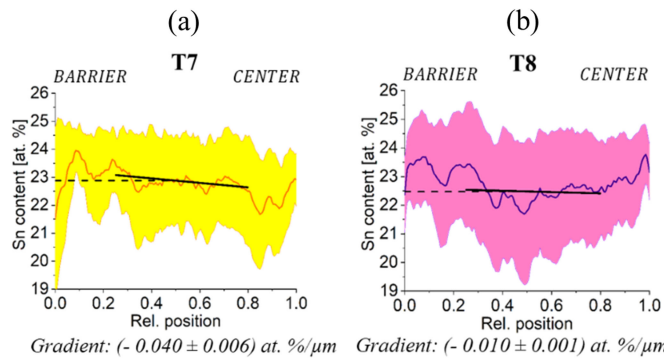


Fig. 6. Sn concentration gradients along the radial direction of T7 (a) and T8 (b). The background, yellow and pink for T7 and T8 respectively, stems from the single measurements performed over several clusters. The dashed lines represent the average Sn content [at%] value taken at 0.5.

to suggest that these six free diffusion routes help Sn to better flow towards the sub-element periphery and homogeneously distribute over the initial Cu matrix. According to this hypothesis, the Nb-free routes, together with the specific heat treatment performed ( $380^\circ\text{C}$  - 48 h,  $580^\circ\text{C}$  - 48 h,  $700^\circ\text{C}$  - 92 h), can lead the Sn content in the most peripheral part of the sub-element to be very close to that of the region near the core.

For this to be confirmed, it would be useful to additionally investigate the kinetics of  $\text{Nb}_3\text{Sn}$  growth at the different heat treatment stages. In this regard, the study by M. V. Krylova *et al.* [15] showed that such Nb-free Cu channels help to accelerate the formation of the superconducting phase by intensifying the diffusion of Sn. However, the role of these resistive separators in contributing to a balance between the Sn concentration near the core and that near the periphery has to be better understood.

Despite the smaller Sn gradient in the case of T8, the average Sn content taken at 0.5 is slightly higher for T7 at the limit of the measurement accuracy. Moreover, the Sn content value near the core is very similar in both wires. It is then difficult to conclude which heat treatment is more effective for obtaining a cluster wire with higher superconducting performance.

Previous analyses on other six-cluster layouts suggested a less homogeneous Sn distribution than found here for T7 and T8 [9]. The behaviour clearly depends sensitively on sub-element design, deformed geometry and heat treatment conditions, and further study is needed to confirm the best approach for optimizing superconducting performance.

### B. T3 Sn Concentration Gradient By TEM-EDX

Fig. 7 shows that the Sn concentration gradient over the  $\text{Nb}_3\text{Sn}$  grains is very small within the experimental margin of error.

Therefore, this preliminary TEM investigation seems to confirm that the cluster layout has an interesting potential for obtaining more homogeneous wires.

### C. T3 Local Transport Properties

The T3 sample was fully magnetized and then scanned in self-field. By inverting the obtained remanent field profile it is possible to evaluate how each sub-element contributes to the local current flow over the cross-section (Fig. 8).

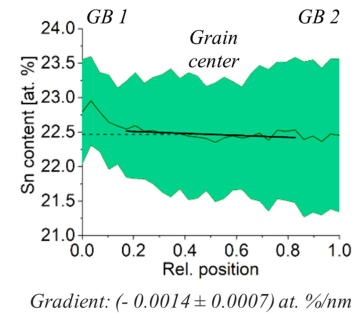


Fig. 7. Sn gradient for a T3 TEM-lamella sample. The coloured background stems from the single measurements performed over several grains. The dashed line represents the average Sn content [at%] value taken at 0.5.

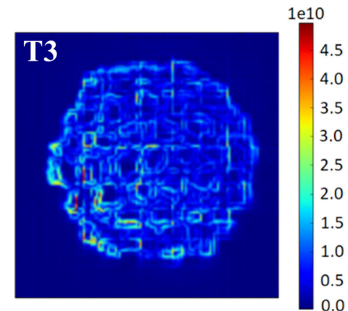


Fig. 8. T3 current densities profile at 10 K and self-field.

The maximum values achieved are in line with the commercial RRP wires (HL-LHC target) at the same conditions (about  $4.8 \times 10^4 \text{ A/mm}^2$ ). Considering the strongly deformed sub-element shapes, also leading the Cu resistive separators to be too thin, and the irregularities of the barriers (Nb, Ta), there is still room for improvements.

The  $J_c$  values can thus be raised by acting on the manufacturing process and heat treatment parameters.

## IV. CONCLUSION

The EDX results observed for the cluster layout samples suggest a high potential in terms of radial homogeneity. Catalyzing Sn diffusion through the Nb-free Cu channels towards the peripheral barrier can therefore be an effective way to be better explored in order to produce wires with a more homogeneous Sn distribution, an optimized average Sn content, and a resulting higher superconducting performance. Moreover, the local currents evaluated from SHPM show a  $J_c$  consistent with the HL-LHC standards, which can be further improved by acting on the manufacturing process steps and the heat treatment parameters.

## ACKNOWLEDGMENT

The construction and production technology of the studied wires were developed at the Bochvar Institute, Russia. The wires were produced at the Chepetsky mechanical plant with the scientific and technological support of the Bochvar Institute. Finally, the first author A. Moros would like to thank J. Gruber and M. Binder for the help with the sample preparation at USTEM, TU Wien.

## REFERENCES

- [1] F. C. C. Collaboration, “FCC-hh: The hadron collider: Future circular collider conceptual design report volume 3,” *Eur. Phys. J. Spec. Top.*, vol. 228, no. 4, pp. 755–1107, Jul. 2019.
- [2] A. Ballarino and L. Bottura, “Targets for R&D on Nb<sub>3</sub>Sn conductor for high energy physics,” *IEEE Trans. Appl. Supercond.*, vol. 25, no. 3, Jun. 2015, Art. no. 6000906.
- [3] R. Flükiger, D. Uglietti, C. Senatore, and F. Buta, “Microstructure, composition and critical current density of superconducting Nb<sub>3</sub>Sn wires,” *Cryogenics*, vol. 48, no. 7-8, pp. 293–307, Jul. 2008.
- [4] A. Godeke, A. Den Ouden, A. Nijhuis, and H. H. J. ten Kate, “State of the art powder-in-tube niobium–tin superconductors,” *Cryogenics*, vol. 48, no. 7-8, pp. 308–316, Jul. 2008.
- [5] T. Baumgartner, J. Hecher, J. Bernardi, S. Pfeiffer, C. Senatore, and M. Eisterer, “Assessing composition gradients in multifilamentary superconductors by means of magnetometry methods,” *Supercond. Sci. Technol.*, vol. 30, no. 1, Nov. 2016, Art. no. 014011.
- [6] B. A. Zeitlin, E. Gregory, T. Pyon, R. M. Scanlan, A. A. Polyanskii, and P. J. Lee, “Progress on the use of internal fins as barriers to reduce magnetization on high current density mono element internal tin conductors (MEIT),” *AIP Conf. Proc.*, vol. 711, no. 1, pp. 417–424, Jun. 2004.
- [7] A. Z. Bruce, “A high current density low cost Nb<sub>3</sub>Sn titanium doped conductor utilizing a novel internal tin process,” Supergenics LLC, Jefferson, MA, USA, Rep. no. INIS-US0683, Feb. 2005. [Online]. Available: <https://www.osti.gov/servlets/purl/837021>
- [8] E. Gregory, “Final report SBIR Phase II. High current density, ( $J_c$ ), low AC loss, low cost, Internal-Tin Superconductor,” Supergenics I LLC, Jefferson, MA, USA, Rep. no. DOE/ER83541, Jan. 2009. [Online]. Available: <https://www.osti.gov/servlets/purl/946132>
- [9] P. A. Lukyanov *et al.*, “The comparative study of the internal tin Nb<sub>3</sub>Sn wires with different layouts,” *J. Phys. Conf. Ser.*, vol. 1559, no. 1, Jun. 2020, Art. no. 012061.
- [10] N. J. Pugh, J. E. Evetts, and E. R. Wallach, “A transmission electron microscopy study of bronze-processed Nb<sub>3</sub>Sn and (Nb,Ta)<sub>3</sub>Sn multifilamentary superconducting wire,” *J. Mater. Sci.*, vol. 20, no. 12, pp. 4521–4526, Dec. 1985.
- [11] V. Abächerli *et al.*, “The influence of Ti doping methods on the high field performance of (Nb,Ta,Ti)<sub>3</sub>Sn multifilamentary wires using Osprey bronze,” *IEEE Trans. Appl. Supercond.*, vol. 15, no. 2, pp. 3482–3485, Jun. 2005.
- [12] C. Senatore *et al.*, “Phase formation, composition and  $T_c$  distribution of binary and Ta-alloyed Nb<sub>3</sub>Sn wires produced by various techniques,” *IEEE Trans. Appl. Supercond.*, vol. 22, no. 3, Dec. 2011, Art. no. 6001304.
- [13] A. Ballarino *et al.*, “The CERN FCC conductor development program: A worldwide effort for the future generation of high-field magnets,” *IEEE Trans. Appl. Supercond.*, vol. 29, no. 5, Jan. 2019, Art. no. 6001709.
- [14] M. Suenaga, D. O. Welch, R. L. Sabatini, O. F. Kammerer, and S. Okuda, “Superconducting critical temperatures, critical magnetic fields, lattice parameters, and chemical compositions of “bulk” pure and alloyed Nb<sub>3</sub>Sn produced by the bronze process,” *J. Appl. Phys.*, vol. 59, no. 3, pp. 840–853, Feb. 1986.
- [15] M. V. Krylova *et al.*, “The microstructure of Nb<sub>3</sub>Sn superconductors differing in the number of copper inserts at various stages of heat treatment,” *Mater. Sci. Eng. Conf. Ser.*, vol. 502, no. 1, Apr. 2019, Art. no. 012174.